

## Investigating the Formation of Giant $\{\text{Pd}_{72}\}^{\text{Prop}}$ and $\{\text{Pd}_{84}\}^{\text{Gly}}$ Macrocycles Using NMR, HPLC, and Mass Spectrometry

Lorna G. Christie, Silke Asche, Jennifer S. Mathieson, Laia Vilà-Nadal, and Leroy Cronin\*<sup>1</sup>

WestCHEM, School of Chemistry, University of Glasgow, Glasgow G12 8QQ, U.K.

### Supporting Information

**ABSTRACT:** The formation of giant polyoxometalate (POM) species is relatively underexplored, as their self-assembly process is complex due to the rapid kinetics. Polyoxopalladates (POPds) are a class of POMs based on Pd, the largest of which is the  $\{\text{Pd}_{84}\}^{\text{Ac}}$  wheel, and its slower kinetics mean the system is more amenable to systematic study. Here, we show that it is possible to follow the assembly of two types of Pd wheels,  $\{\text{Pd}_{84}\}^{\text{Gly}}$  and the smaller  $\{\text{Pd}_{72}\}^{\text{Prop}}$ , formed using glycolate and propionate ligands, respectively. We analyzed the formation of  $\{\text{Pd}_{72}\}^{\text{Prop}}$  and  $\{\text{Pd}_{84}\}^{\text{Gly}}$  using mass spectrometry (SEC-HPLC-MS and preparative desalting followed by MS). This was accompanied by studies that followed the chemical shift differences between the outer/inner ligands and the free ligand in solution for the  $\{\text{Pd}_{84}\}^{\text{Ac}}$ ,  $\{\text{Pd}_{72}\}^{\text{Prop}}$ , and  $\{\text{Pd}_{84}\}^{\text{Gly}}$  species using NMR, which showed it was possible to track the formation of the wheels. Our findings confirm that the macrocycles assemble from smaller building blocks that react together to form the larger species over a period of days. These findings open the way for further structural derivatives and exploration of their host–guest chemistry.

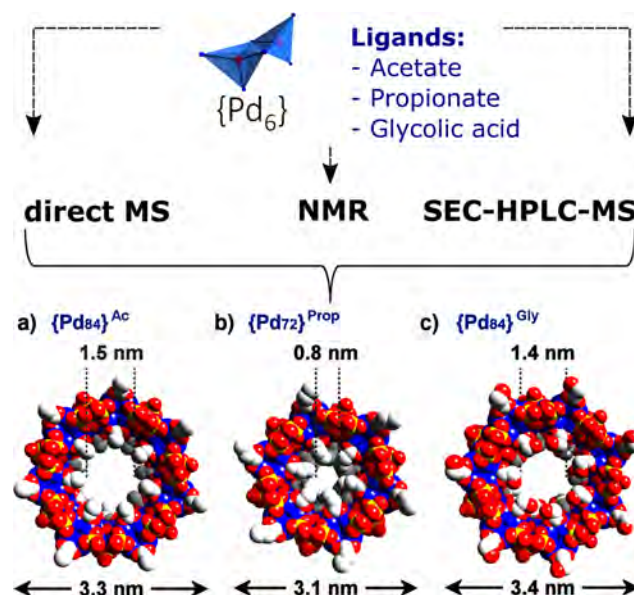


**Figure 1.** Scheme showing the studies done to explore the self-assembly of the palladium-based macrocycles, shown in space filling representation, with the corresponding overall and inner cavity diameters. Pd, blue; O, red; P, yellow; C, gray.

Polyoxometalates (POMs) are metal oxide clusters formed by transition metals like Mo, V, and W that are able to self-assemble in complex, high-nuclearity structures from simple precursors.<sup>1</sup> Noble metals Pd, Pt, and Au, and even lanthanides like Ga, can form high-nuclearity metal oxide structures, such as wheel-like  $\{\text{Gd}_{140}\}$ .<sup>2,3</sup> One of the challenges in this field is to understand the assembly process, especially for the systems that form gigantic ring clusters, and only a few mechanistic studies have been explored. These studies have been limited due to the rapid kinetics,<sup>4</sup> and mechanistic data have been restricted to low-nuclearity moieties.<sup>5–8</sup> However, the formation of curved units is suggested to be the driving force in the formation of both spherical molybdenum brown Keplerate  $\{\text{Mo}_{132}\}$ <sup>9–12</sup> and ring-shaped molybdenum blue ring  $\{\text{Mo}_{154}\}$ .<sup>13</sup>

To address this issue, we decided to target systems that form gigantic structures but assemble more slowly.<sup>14,15</sup> The first of these is a smaller  $\{\text{Pd}_{72}\}^{\text{Prop}}$  wheel of general formula  $\text{Na}_{60}[\text{Pd}_{72}\text{O}_{36}(\text{C}_2\text{H}_5\text{CO}_2)_{24}(\text{PO}_4)_{36}] \cdot 200\text{H}_2\text{O}$ , containing 24 bridging propionate ligands. The second is an exact structural analogue of the original  $\{\text{Pd}_{84}\}^{\text{Ac}}$  wheel,<sup>14</sup> denoted  $\{\text{Pd}_{84}\}^{\text{Gly}}$ , of general formula  $\text{Na}_{56}\text{H}_{14}[\text{Pd}_{84}\text{O}_{42}(\text{CH}_2\text{CO}_3)_{28}(\text{PO}_4)_{42}] \cdot 200\text{H}_2\text{O}$  (Figure 1). This structural analogue contains 28

glycolate ligands in place of acetate. To directly probe the mechanisms of formation of the  $\{\text{Pd}_{72}\}^{\text{Prop}}$  and  $\{\text{Pd}_{84}\}^{\text{Gly}}$  *in situ*, we used mass spectrometry (MS) and <sup>1</sup>H NMR. However, MS cannot be used to follow the process in the reaction solutions directly due to ion suppression issues arising from the high salt concentration. Therefore, we developed a separation “desalting” step. To do this we used SEC-HPLC-MS to separate the species present in the reaction based on their size. The second method was the direct injection of aliquots of mother liquor which had been prepared by “desalting” in small disposable size-exclusion columns (MicroBioSpin 6).

Preliminary studies had suggested that the manual desalting columns are more effective at removing salt from the Pd macrocycle reaction mother liquor, and therefore give higher quality mass spectra, see Figure 2 and Table 1. Furthermore, initial observations had also suggested that the  $\{\text{Pd}_{72}\}^{\text{Prop}}$  and  $\{\text{Pd}_{84}\}^{\text{Gly}}$  macrocycles are not as stable as  $\{\text{Pd}_{84}\}^{\text{Ac}}$  under SEC-HPLC-MS conditions. Therefore, the desalting technique was employed as a complementary approach to the SEC-HPLC

Received: May 19, 2018

Published: July 13, 2018

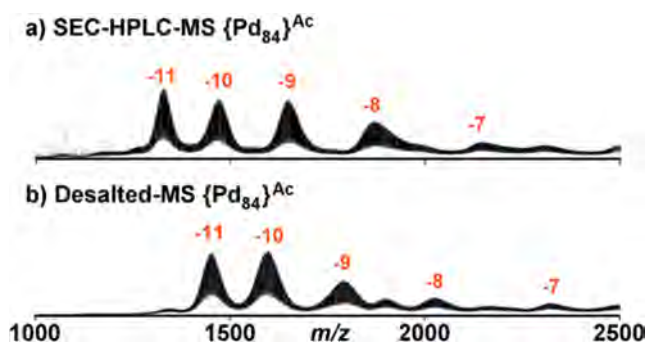


**Figure 2.** Mass spectra of pure crystalline  $\{Pd_{84}\}^{Ac}$  obtained by (a) SEC-HPLC-MS and (b) preparative desalting followed by direct injection into the mass spectrometer.

**Table 1. Simplified Mass Spectra Assignments of Crystalline  $\{Pd_{84}\}^{Ac}$  Analyzed Using (a) SEC-HPLC-MS and (b) Preparative Desalting + MS (Ac = Acetate Ligand)**

z	m/z		assignment
	obs	calc	
(a) SEC-HPLC-MS			
-11	1328	1328.1	$\{Pd_{84}O_{42}(Ac)_{16}(PO_4)_{42}\}^{11-}$
-10	1470	1469.6	$\{Pd_{84}O_{42}(Ac)_{17}(PO_4)_{42}\}^{10-}$
-9	1648	1648.2	$\{Pd_{84}O_{42}(Ac)_{20}(PO_4)_{42}\}^{9-}$
-8	1867	1866.8	$\{Pd_{84}O_{42}(Ac)_{21}(PO_4)_{42}\}^{8-}$
-7	2147	2147.7	$\{Pd_{84}O_{42}(Ac)_{23}(PO_4)_{42}\}^{7-}$
(b) Desalting + MS			
-11	1450	1449.9	$\{Pd_{84}O_{42}(Ac)_{28}(PO_4)_{42}\}^{11-}$
-10	1595	1595.0	$\{Pd_{84}O_{42}(Ac)_{28}(PO_4)_{42}\}^{10-}$
-9	1790	1789.0	$\{Pd_{84}O_{42}(Ac)_{28}(PO_4)_{42}\}^{9-}$
-8	2023	2023.3	$\{Pd_{84}O_{42}(Ac)_{28}(PO_4)_{42}\}^{8-}$
-7	2323	2323.0	$\{Pd_{84}O_{42}(Ac)_{28}(PO_4)_{42}\}^{7-}$

method. Initially, a direct comparison of the two MS techniques was carried out on pure crystalline  $\{Pd_{84}\}^{Ac}$ . Aliquots of identical solutions of the crystalline  $\{Pd_{84}\}^{Ac}$  (conc  $\sim 20$  mg/mL) were analyzed by SEC-HPLC-MS and by passing the sample through the desalting columns followed by direct injection into the mass spectrometer. This showed that 5–12 ligands were removed from the macrocycle. Conversely, the assignments for the sample of  $\{Pd_{84}\}^{Ac}$ , which was manually desalted, revealed a fully intact wheel (28 acetate ligands) across all the charge states (Table 1).

We propose that the observed ligand loss when the sample undergoes SEC-HPLC is due to partial breakdown of the wheel in pure water, suggesting  $\{Pd_{84}\}^{Ac}$  has limited stability in pure water. This is consistent with  $^1H$  NMR experiments on pure  $\{Pd_{84}\}^{Ac}$  in  $D_2O$ , which reveal dissociation of the acetate ligands (Supporting Information (SI), Figure S1). This is because the desalting procedure is a “softer” method of sample preparation than SEC-HPLC-MS in which the sample travels through a significantly shorter column, is not under pressure, and is not mixed with water for a prolonged period of time. Hence,  $\{Pd_{84}\}^{Ac}$  remains fully intact when analyzed using this method. Table 1 shows the simplified assignments for SEC-HPLC-MS vs desalting + MS of  $\{Pd_{84}\}^{Ac}$ , showing the number of acetate (Ac) ligands present in each case (counterions and associated water molecules have been omitted for clarity; full assignments can be found in SI, Table S1). Having established the difference between the SEC-HPLC-MS and manual

desalting methods. We carried out experiments using both of these techniques to analyze the formation of  $\{Pd_{72}\}^{Prop}$  and  $\{Pd_{84}\}^{Gly}$ . Unexpectedly, the SEC-HPLC-MS study of the  $\{Pd_{72}\}^{Prop}$  synthesis showed no products with  $m/z > 1300$ . However, all the spectra contained peaks at  $m/z \sim 1100$  and 764, which can be assigned as  $\{[Pd_6O_{2-4}(C_3H_5O_2)_{1-4}(PO_4)_{2-4}]Na_xH_y(H_2O)_z\}^-$  and  $\{[Pd_{12}O_{5-7}(C_3H_5O_2)_{4-6}(PO_4)_{5-7}]Na_xH_y(H_2O)_z\}^{3-}$ , respectively, corresponding to the propionate analogues of the  $\{Pd_6\}$  and  $\{Pd_{12}\}$  subunits. Conversely, the mass spectra obtained through the preparative desalting technique revealed a fully intact  $\{Pd_{72}\}^{Prop}$  wheel present in solution from day 5 onward (Figure 2b), consistent with an increasing concentration of the macrocycle in solution.

We also wanted to assess the formation of  $\{Pd_{72}\}^{Prop}$  and  $\{Pd_{84}\}^{Gly}$  via SEC-HPLC alone; for synthetic procedures see the SI. This was a particularly interesting experiment because both  $\{Pd_{72}\}^{Prop}$  and  $\{Pd_{84}\}^{Gly}$  appeared to break down completely during SEC-HPLC-MS when water was used as the mobile phase. On day 1 of the  $\{Pd_{72}\}^{Prop}$  reaction, a small shoulder peak could be detected around 19.4 min in the SEC trace, which grows in intensity and sharpens over time, resulting in another distinct peak at 19.2 min on day 4, see Figure 3a.

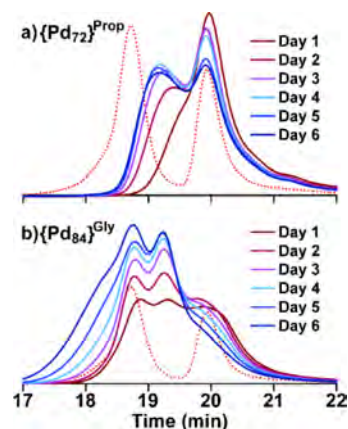


**Figure 3.** SEC-HPLC chromatograms (eluting with 0.05 M NaOAc solution) recorded on days 1–6 of (a)  $\{Pd_{72}\}^{Prop}$  mother liquor and (b)  $\{Pd_{84}\}^{Gly}$  mother liquor, plotted against a 1:1 mix of  $\{Pd_{84}\}^{Ac}$  and  $\{Pd_{15}\}$  for size comparison.

The retention time of this species corresponds to what is expected for the  $\{Pd_{72}\}^{Prop}$  wheel,<sup>15</sup> and the emergence of the small shoulder peak, which grows over the course of this study, is further evidence to suggest that the  $\{Pd_{72}\}^{Prop}$  wheel forms whereby the small building units aggregate to form the final macrocyclic structure. The mother liquor for  $\{Pd_{84}\}^{Gly}$  was also analyzed by SEC-HPLC alone, see Figure 3. Two peak maxima can be seen at 19.3 and  $\sim 18.8$  min, which grow in intensity over days 1–6. The peak at 18.8 min corresponds to  $\{Pd_{84}\}^{Gly}$  and can be seen to shift gradually to a lower retention time from day 1 through day 4. Interestingly, the peak at 19.3 min, which is between the sizes of those of  $\{Pd_{15}\}$  and  $\{Pd_{84}\}^{Ac}$ , is thought to correspond to the  $\{Pd_{30}\}$  species observed in SEC-HPLC-MS. The  $\{Pd_{84}\}^{Gly}$  wheel and the  $\{Pd_{30}\}$  species are present in solution simultaneously, which could indicate that  $\{Pd_{30}\}$  behaves as an intermediate or template in the self-assembly process.

Complementary to the MS study,  $^1H$  NMR experiments were conducted on the mother liquor to explore the self-

assembly of the Pd wheels. Here  $^1\text{H}$  NMR was used directly to follow the change of chemical shift of the carboxylic ligands that are necessary for the assembly of  $\{\text{Pd}_{72}\}^{\text{Prop}}$ ,  $\{\text{Pd}_{84}\}^{\text{Ac}}$ , and  $\{\text{Pd}_{84}\}^{\text{Gly}}$  macrocycles in solution. The signal at 1.63 ppm corresponds to the 14 acetate ligands located inside the  $\text{Pd}_{84}$  wheel; this signal is shifted compared to that of the free acetate in solution (1.73 ppm). The smaller intensity peak corresponds to the 14 acetate ligands located outside the  $\text{Pd}_{84}$  wheel (2.21 ppm) and indicates a change in the electronic environment of the ligand inside the wheel compared to the free acetate in solution, see Figure 4.

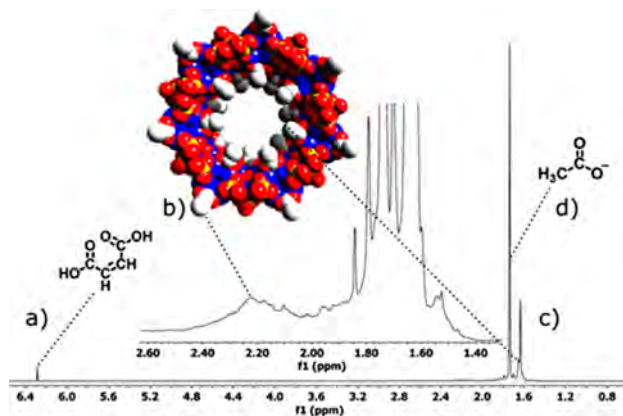


**Figure 4.**  $^1\text{H}$  NMR spectra of  $\{\text{Pd}_{84}\}^{\text{Ac}}$ , general formula  $[\text{Pd}_{84}\text{O}_{42}(\text{PO}_4)_{42}(\text{CH}_3\text{CO}_2)_{28}]^{70-}$ , mother liquor at day 10: (a) maleic acid standard (6.28 ppm), (b) outer acetate (2.21 ppm), (c) inner acetate (1.63 ppm), and (d) free acetate in solution (1.73 ppm).

This is similar to that found for the inclusion guests within the spherical  $\{\text{Mo}_{132}\}$ .<sup>9,10</sup> The chemical shift differences observed in  $\{\text{Pd}_{84}\}^{\text{Ac}}$  between the outer or inner acetates and the free acetate in solution allowed quantification of the amount of the free versus inner acetate in Pd wheel synthesis. Similar differences were seen for the  $\{\text{Pd}_{72}\}^{\text{Prop}}$  and  $\{\text{Pd}_{84}\}^{\text{Gly}}$  species, see SI, and the percentage of inner/free ligands in the mother liquor solution was determined from the intensity ratio of the  $^1\text{H}$  NMR resonance, see Figure 5 and see SI for  $\{\text{Pd}_{84}\}^{\text{Gly}}$ . The results show a 30% decrease of the free acetate in solution over the 10 day period in the case of  $\{\text{Pd}_{84}\}^{\text{Ac}}$ , and a smaller 10% decrease of free propionate for  $\{\text{Pd}_{72}\}^{\text{Prop}}$ .

The  $^1\text{H}$  NMR results combined with the two different mass spectrometry techniques (SEC-HPLC-MS and desalting followed by MS) were used to study the buildup mechanism of  $\{\text{Pd}_{72}\}^{\text{Prop}}$  and  $\{\text{Pd}_{84}\}^{\text{Gly}}$  over 10 days. Initial studies showed that the SEC-HPLC process caused loss of acetate ligands from  $\{\text{Pd}_{84}\}^{\text{Ac}}$ . This was verified by carrying out a comparative study on a pure sample of  $\{\text{Pd}_{84}\}^{\text{Ac}}$  crystals analyzed using both MS methods. This ligand loss was attributed to the instability of  $\{\text{Pd}_{84}\}^{\text{Ac}}$  in water (the mobile phase used in SEC-HPLC-MS). SEC-HPLC-MS revealed no clear signals in the mass spectra at  $m/z > 1300$  for the  $\{\text{Pd}_{72}\}^{\text{Prop}}$  reaction. This was attributed to its rapid water loss during the SEC-HPLC process, which had already been seen to occur to a lesser extent with  $\{\text{Pd}_{84}\}^{\text{Ac}}$ . Despite this,  $\{\text{Pd}_6\}^{\text{Prop}}$  and  $\{\text{Pd}_{12}\}^{\text{Prop}}$  building blocks were detected throughout the study. The mass spectra obtained through desalting the  $\{\text{Pd}_{72}\}^{\text{Prop}}$  mother liquor revealed the presence of a fully intact  $\{\text{Pd}_{72}\}^{\text{Prop}}$  wheel from day 5 onward. SEC-HPLC was consistent with the desalting MS, showing a

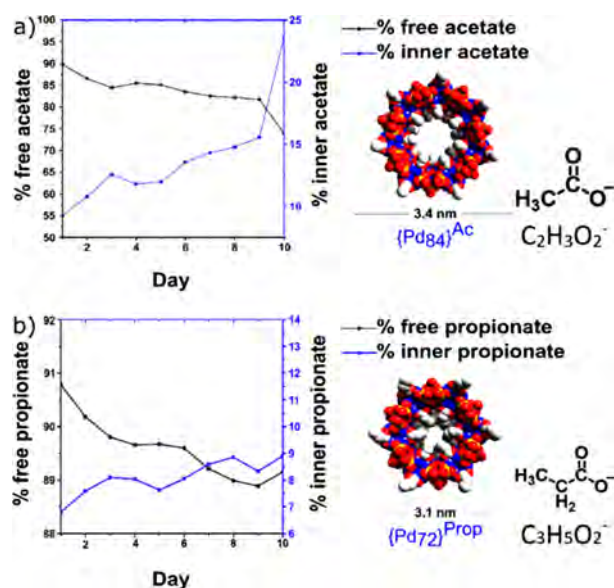


**Figure 5.**  $^1\text{H}$  NMR data comparison of the % free ligand (acetate or propionate) versus the % inner ligand in the mother liquor, 10 day buildup of (a)  $\{\text{Pd}_{84}\}^{\text{Ac}}$  and (b)  $\{\text{Pd}_{72}\}^{\text{Prop}}$ .

peak at retention time 19.2 min on day 5 corresponding to  $\{\text{Pd}_{72}\}^{\text{Prop}}$ : this peak is seen to emerge over the 6 day study.

Overall, we can conclude that  $\{\text{Pd}_{72}\}^{\text{Prop}}$  takes 5 days to form in solution, and the presence of  $\{\text{Pd}_6\}^{\text{Prop}}$  and  $\{\text{Pd}_{12}\}^{\text{Prop}}$  could indicate a buildup regime similar to that of  $\{\text{Pd}_{84}\}^{\text{Ac}}$ . Using the desalting technique,  $\{\text{Pd}_{84}\}^{\text{Gly}}$  was found to form in solution after 4 days. Similar to the  $\{\text{Pd}_{72}\}^{\text{Prop}}$  study, SEC-HPLC-MS was unable to identify the intact  $\{\text{Pd}_{84}\}^{\text{Gly}}$  wheel on any day of the study. However, the spectra showed a  $\{\text{Pd}_6\}^{\text{Gly}}$  unit which decreased in intensity over time, suggesting this could be the building block which is gradually consumed as it assembles into larger species. Finally, we also found that the SEC-HPLC-MS spectra also showed the presence of a  $\{\text{Pd}_{30}\}$  species; this was detected from day 1 and from day 4 through day 10, and can also be detected by SEC-HPLC alone. Thus, we postulate this unit could act as a template, indicating that the rings are built via gradual chain elongation in solution, as described in Figure 6.

In summary, we have used a combination of techniques to explore the assembly of gigantic polyoxopalladates, and this

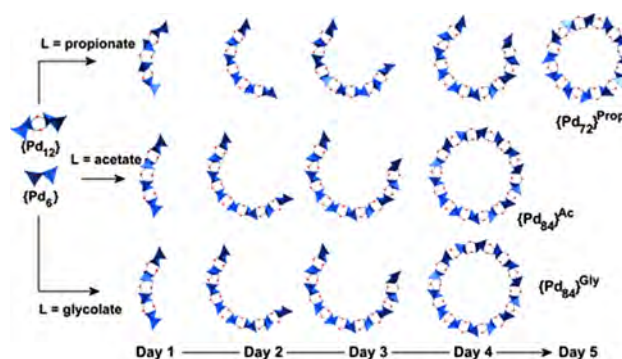


**Figure 6.** General mechanism of assembly for three giant POPds,  $\{\text{Pd}_{72}\}^{\text{Prop}}$ ,  $\{\text{Pd}_{84}\}^{\text{Ac}}$ , and  $\{\text{Pd}_{84}\}^{\text{Gly}}$ , suggested by our spectroscopic studies. The scheme depicts the chains as unconnected, but equally the smaller chains might be able to be connected and ring expansion with further building blocks could occur.

allowed us to follow the formation of the rings in solution, which suggested a common mechanism. Compared to the self-assembly of the {Mo<sub>154</sub>} wheel family,<sup>13</sup> this system requires much more time (from less than a second to several days). Also, the possibility of a ring-expansion rather than chain-growth mechanism might be considered, given the nature of the kinetics for the assembly of Pd systems. Further studies exploring the nature of the {Pd<sub>30</sub>} species as a possible template or building block are ongoing.

## ■ ASSOCIATED CONTENT

### 📄 Supporting Information

The Supporting Information is available free of charge on the ACS Publications website at DOI: 10.1021/jacs.8b05059.

Experimental details; full mass spectra and assignments (PDF)

## ■ AUTHOR INFORMATION

### Corresponding Author

\*lee.cronin@glasgow.ac.uk

### ORCID

Leroy Cronin: 0000-0001-8035-5757

### Notes

The authors declare no competing financial interest.

## ■ ACKNOWLEDGMENTS

The authors gratefully acknowledge financial support from the EPSRC (Grant Nos. EP/H024107/1, EP/K023004/1, EP/K038885/1, EP/L023652/1), BBSRC (Grant No. BB/M011267/1), and the EC project MICREAGENTS, ERC (project 670467 SMART-POM).

## ■ REFERENCES

- (1) Long, D.-L.; Tsunashima, R.; Cronin, L. *Angew. Chem., Int. Ed.* **2010**, *49* (10), 1736–1758.
- (2) Izarova, N. V.; Pope, M. T.; Kortz, U. *Angew. Chem., Int. Ed.* **2012**, *51* (38), 9492–9510.
- (3) Zheng, X. Y.; Jiang, Y. H.; Zhuang, G. L.; Liu, D. P.; Liao, H. G.; Kong, X. J.; Long, L. S.; Zheng, L. S. *J. Am. Chem. Soc.* **2017**, *139* (50), 18178–18181.
- (4) Miras, H. N.; Cooper, G. J. T.; Long, D.-L.; Bögge, H.; Müller, A.; Streb, C.; Cronin, L. *Science* **2010**, *327* (5961), 72–74.
- (5) Vilà-Nadal, L.; Mitchell, S. G.; Rodríguez-Fortea, A.; Miras, H. N.; Cronin, L.; Poblet, J. M. *Phys. Chem. Chem. Phys.* **2011**, *13* (45), 20136–20145.
- (6) Vilà-Nadal, L.; Wilson, E. F.; Miras, H. N.; Rodríguez-Fortea, A.; Cronin, L.; Poblet, J. M. *Inorg. Chem.* **2011**, *50* (16), 7811–7819.
- (7) Biswas, S.; Melgar, D.; Srimany, A.; Rodríguez-Fortea, A.; Pradeep, T.; Bo, C.; Poblet, J. M.; Roy, S. *Inorg. Chem.* **2016**, *55* (17), 8285–8291.
- (8) Vilà-Nadal, L.; Rodríguez-Fortea, A.; Yan, L. K.; Wilson, E. F.; Cronin, L.; Poblet, J. M. *Angew. Chem., Int. Ed.* **2009**, *48* (30), 5452–5456.
- (9) Ziv, A.; Grego, A.; Kopilevich, S.; Zeiri, L.; Miró, P.; Bo, C.; Müller, A.; Weinstock, I. A. *J. Am. Chem. Soc.* **2009**, *131* (18), 6380–6382.
- (10) Lai, T. L.; Awada, M.; Floquet, S.; Roch-Marchal, C.; Watfa, N.; Marrot, J.; Haouas, M.; Taulelle, F.; Cadot, E. *Chem. - Eur. J.* **2015**, *21* (38), 13311–13320.
- (11) Watfa, N.; Haouas, M.; Floquet, S.; Hijazi, A.; Naoufal, D.; Taulelle, F.; Cadot, E. *Inorg. Chem.* **2016**, *55*, 9368–9376.
- (12) Watfa, N.; Melgar, D.; Haouas, M.; Taulelle, F.; Hijazi, A.; Naoufal, D.; Avalos, J. B.; Floquet, S.; Bo, C.; Cadot, E. *J. Am. Chem. Soc.* **2015**, *137* (17), 5845–5851.

(13) Liu, T.; Diemann, E.; Li, H.; Dress, A. W. M.; Müller, A. *Nature* **2003**, *426*, 59–62.

(14) Xu, F.; Miras, H. N.; Scullion, R. A.; Long, D.-L.; Thiel, J.; Cronin, L. *Proc. Natl. Acad. Sci. U. S. A.* **2012**, *109* (29), 11609–11612.

(15) Scullion, R. A.; Surman, A. J.; Xu, F.; Mathieson, J. S.; Long, D.-L.; Haso, F.; Liu, T.; Cronin, L. *Angew. Chem., Int. Ed.* **2014**, *53* (38), 10032–10037.